nature genetics



# Inversin, the gene product mutated in nephronophthisis type II, functions as a molecular switch between Wnt signaling pathways

Matias Simons[1,6], Joachim Gloy[1,6], Athina Ganner[1], Axel Bullerkotte[1], Mikhail Bashkurov[1], Corinna Krönig[1], Bernhard Schermer[1], Thomas Benzing[1], Olga A Cabello[2], Andreas Jenny[3], Marek Mlodzik[3], Bozena Polok[4], Wolfgang Driever[4], Tomoko Obara[5] & Gerd Walz[1]

**Cystic renal diseases are caused by mutations of proteins that share a unique subcellular localization: the primary cilium of tubular epithelial cells[1]. Mutations of the ciliary protein inversin cause nephronophthisis type II, an autosomal recessive cystic kidney disease characterized by extensive renal cysts, *situs inversus* and renal failure[2]. Here we report that inversin acts as a molecular switch between different Wnt signaling cascades. Inversin inhibits the canonical Wnt pathway by targeting cytoplasmic dishevelled (Dsh or Dvl1) for degradation; concomitantly, it is required for convergent extension movements in gastrulating *Xenopus laevis* embryos and elongation of animal cap explants, both regulated by noncanonical Wnt signaling. In zebrafish, the structurally related switch molecule diversin ameliorates renal cysts caused by the depletion of inversin, implying that an inhibition of canonical Wnt signaling is required for normal renal development. Fluid flow increases inversin levels in ciliated tubular epithelial cells and seems to regulate this crucial switch between Wnt signaling pathways during renal development.**

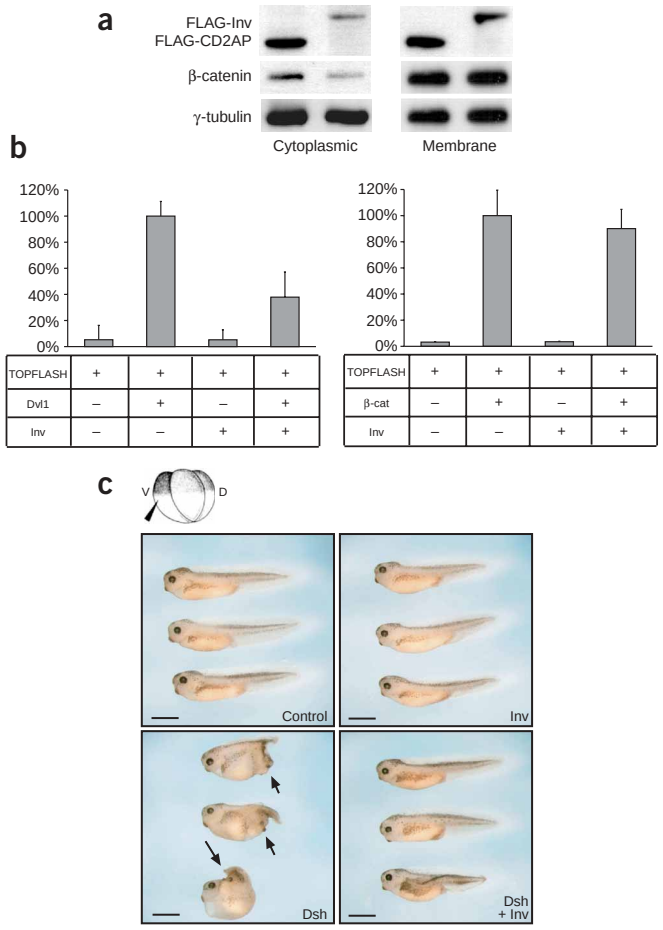


**Figure 1** Inversin inhibits canonical Wnt signaling. (**a**) Expression of inversin reduced endogenous levels of cytoplasmic, but not membrane-bound, β-catenin in HEK 293T cells transiently transfected with Dvl1 and either inversin or a control plasmid (CD2AP). Western blots were reprobed for γ-tubulin as a loading control. (**b**) Inversin blocked Dvl1-induced, but not β-catenin-induced, activation of a TCF/LEF-1–dependent luciferase reporter construct (TOPFLASH) in HEK 293T cells. Experiments were done in triplicate, and data were normalized for β-galactosidase activity. (**c**) Inversin inhibited secondary body axes in *X. laevis* embryos. Embryos were injected with RNA (Inv, inversin) into one ventral blastomere and scored at tadpole stage. The Dsh-induced secondary axes (arrows) were inhibited in the presence of inversin. Scale bars, 1 mm. See also **Table 1**.

[1]Renal Division, University Hospital Freiburg, Hugstetter Strasse 55, 79106 Freiburg, Germany. [2]Department of Molecular and Cellular Biology, Baylor College of Medicine, One Baylor Plaza, Suite 125A, Houston, Texas 77030, USA. [3]Brookdale Department of Molecular, Cell and Developmental Biology, Mount Sinai School of Medicine, One Gustave L. Levy Place, New York, New York 10029, USA. [4]Department of Biology, University of Freiburg, Hauptstrasse 1, 79104 Freiburg, Germany. [5]Department of Medicine, Case Western Reserve University, 2500 MetroHealth Drive, Cleveland, Ohio 44109, USA. [6]These authors contributed equally to this work. Correspondence should be addressed to G.W. (gerd.walz@uniklinik-freiburg.de).

Published online 24 April 2005; doi:10.1038/ng1552

**Table 1 Induction of secondary body axes by RNA microinjection**

| Experimental condition | Body axis score[a] | *n* |
|---|---|---|
| Control | 0 ± 0 | 399 |
| Inversin (1 ng) | 0 ± 0 | 89 |
| Dsh (0.25 ng) | 0.52 ± 0.11 | 31 |
| Dsh (0.25 ng) + inversin (1 ng) | 0.13 ± 0.09[b] | 15 |
| Dsh (0.5 ng) | 1.01 ± 0.05 | 165 |
| Dsh (0.5 ng) + inversin (0.5 ng) | 0.61 ± 0.06[b] | 103 |
| Dsh (0.5 ng) + inversin (1 ng) | 0.30 ± 0.05[b] | 91 |
| Dsh (1 ng) | 1.32 ± 0.05 | 148 |
| Dsh (1 ng) + inversin (1 ng) | 0.95 ± 0.07[b] | 116 |
| Dsh (1 ng) + inversin (2 ng) | 0.75 ± 0.11[b] | 32 |
| CK1ε (0.5 ng) | 1.29 ± 0.06 | 86 |
| CK1ε (0.5 ng) + inversin (1 ng) | 1.06 ± 0.08[b] | 53 |
| CK1ε (0.5 ng) + inversin (2 ng) | 0.60 ± 0.10[b] | 30 |
| CK1ε (0.7 ng) | 1.60 ± 0.09 | 43 |
| CK1ε (0.7 ng) + inversin (1 ng) | 1.28 ± 0.09[b] | 25 |
| β-catenin (100 pg) | 1.17 ± 0.10 | 58 |
| β-catenin (100 pg) + inversin (1 ng) | 1.05 ± 0.07 | 65 |

[a]Mean ± s.e. body axis score using the following scale: 0, no axes; 1, partial secondary axes; 2, complete secondary axes. [b]Statistically significant inhibition of secondary axes by inversin ($P < 0.05$).

Inversin was first identified by positional cloning as a protein of 1,062 amino acids containing an ankyrin repeat deleted in *inv/inv* mutant mice[3,4]. Kidneys of *inv/inv* mice had various developmental abnormalities. In wild-type and heterozygous embryos, nephrogenesis was slowed by embryonic day (E) 17.5 and mature glomeruli congressed at the cortex, whereas *inv/inv* mutants were marked by a persistent cortical nephrogenic zone with abundant immature tubules bearing S- and comma-shaped bodies (**Supplementary Fig. 1** online). The delay in tubular maturation and cyst formation resembles the phenotype of mice with dysregulated Wnt–β-catenin signaling[5,6]. During early kidney development, canonical Wnt signaling is necessary for the induction of metanephric mesenchyme and cell proliferation in branching morphogenesis[7]. At later developmental stages, however, persistent activation of Wnt–β-catenin signaling results in renal cyst formation[5,6]. Because *inv/inv* mice also had hair-pattern changes reminiscent of those in Frizzled6-deficient mice[8] (**Supplementary Fig. 2** online), we speculated that inversin may have a role in Wnt signaling.

In canonical Wnt signaling, Wnt molecules bind to members of the Frizzled receptor protein family to activate dishevelled. This activation inhibits the degradation of β-catenin by the GSK3-β–axin–APC complex. After translocation to the nucleus, β-catenin interacts with TCF family members, activating Wnt target genes[9–12]. Overexpression of inversin in HEK 293T cells facilitated the degradation of cytoplasmic β-catenin (**Fig. 1a**) and blocked Dvl1-mediated activation of TCF-dependent transcription (**Fig. 1b**). Consistent with its effect on TCF-mediated gene activation, inversin inhibited Dsh-mediated double-axis formation when microinjected into *X. laevis* embryos (**Fig. 1c** and **Table 1**). Epistasis analysis showed that inversin antagonized double-axis formation induced by Dsh and by casein kinase 1ε (CK1ε) but not by β-catenin (**Fig. 1c** and **Table 1**) or dominant negative forms of GSK3-β and axin (data not shown).

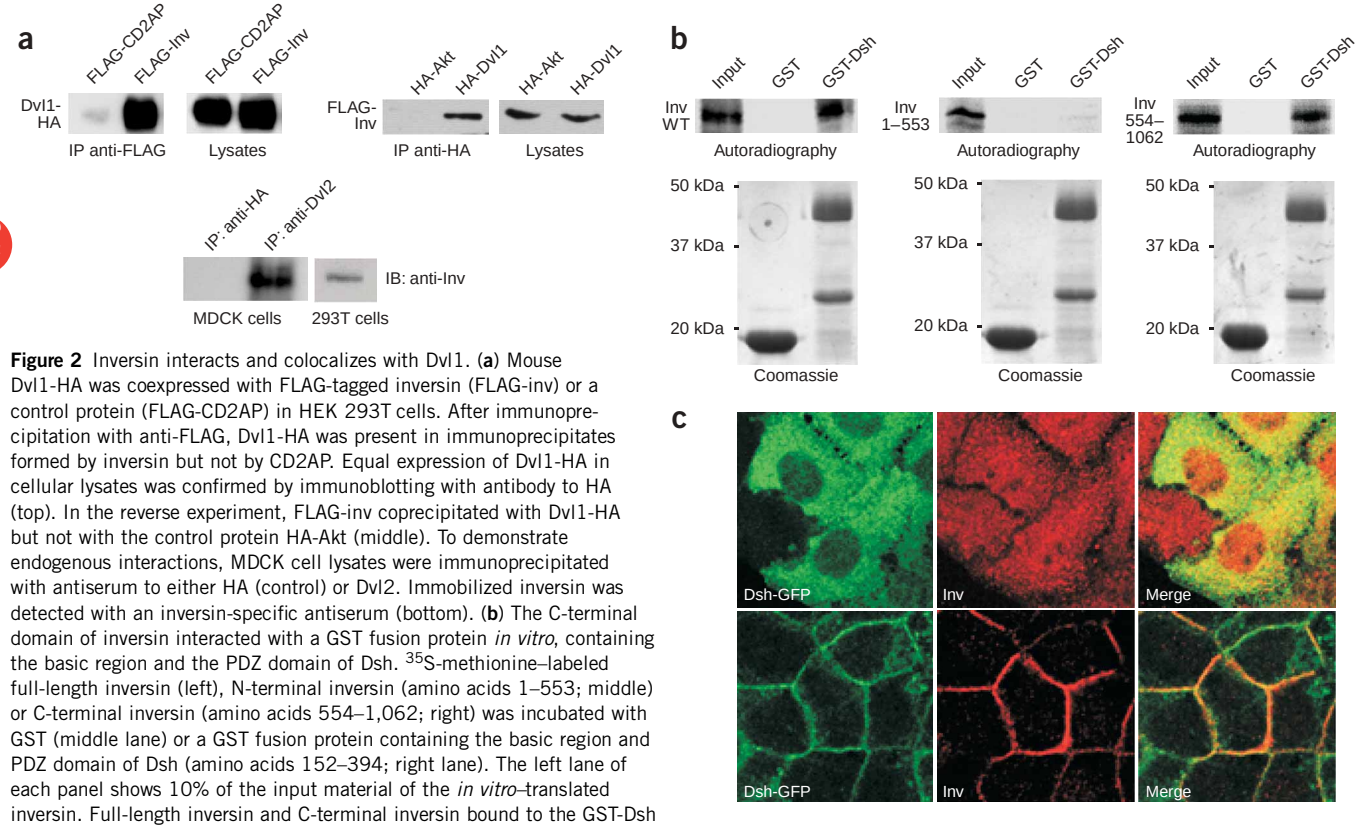


**Figure 2** Inversin interacts and colocalizes with Dvl1. (**a**) Mouse Dvl1-HA was coexpressed with FLAG-tagged inversin (FLAG-inv) or a control protein (FLAG-CD2AP) in HEK 293T cells. After immunoprecipitation with anti-FLAG, Dvl1-HA was present in immunoprecipitates formed by inversin but not by CD2AP. Equal expression of Dvl1-HA in cellular lysates was confirmed by immunoblotting with antibody to HA (top). In the reverse experiment, FLAG-inv coprecipitated with Dvl1-HA but not with the control protein HA-Akt (middle). To demonstrate endogenous interactions, MDCK cell lysates were immunoprecipitated with antiserum to either HA (control) or Dvl2. Immobilized inversin was detected with an inversin-specific antiserum (bottom). (**b**) The C-terminal domain of inversin interacted with a GST fusion protein *in vitro*, containing the basic region and the PDZ domain of Dsh. $^{35}$S-methionine–labeled full-length inversin (left), N-terminal inversin (amino acids 1–553; middle) or C-terminal inversin (amino acids 554–1,062; right) was incubated with GST (middle lane) or a GST fusion protein containing the basic region and PDZ domain of Dsh (amino acids 152–394; right lane). The left lane of each panel shows 10% of the input material of the *in vitro*–translated inversin. Full-length inversin and C-terminal inversin bound to the GST-Dsh fusion protein, whereas N-terminal inversin did not interact with Dsh. Equal amounts of the GST proteins were confirmed by Coomassie staining. (**c**) MDCK cells overexpressing Dsh-GFP were colabeled with a rabbit polyclonal antiserum to inversin at subconfluent (upper row) and confluent stages (lower row). Both inversin and Dsh-GFP translocate to the lateral plasma membrane during differentiation of MDCK cells.

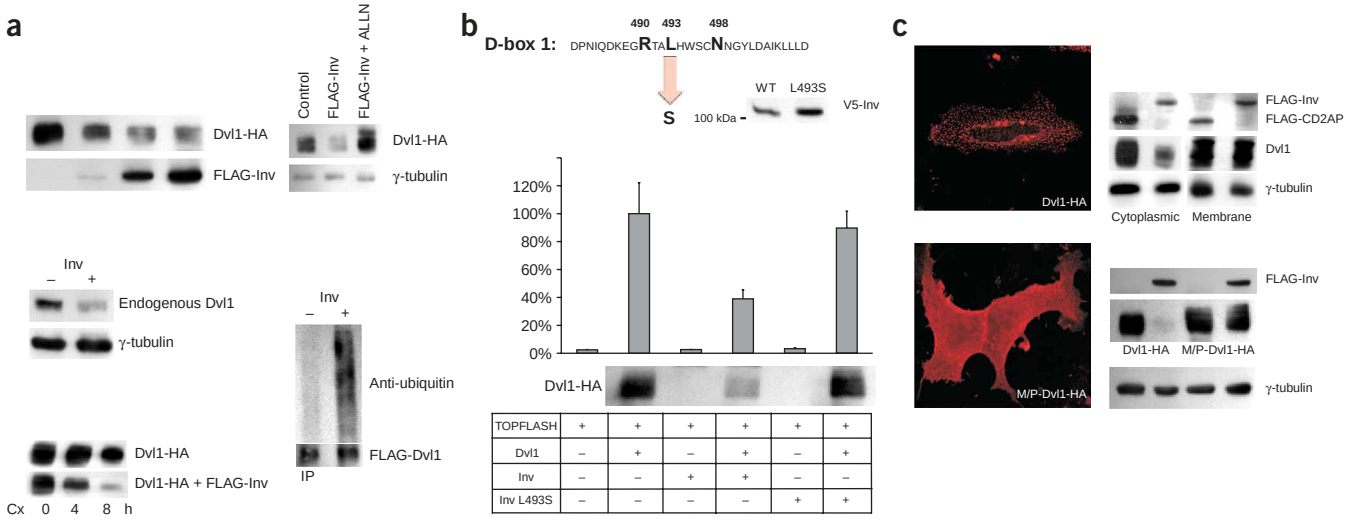


**Figure 3** Inversin facilitates the degradation of Dvl1. (**a**) Levels of both transiently expressed (top left) and endogenous Dvl1 (middle) were reduced in HEK 293T cells expressing inversin. The amount of transfected FLAG-tagged inversin (top left) was 0, 0.1, 1 and 5 μg in lanes 1–4, respectively. The half-life of Dvl1 decreased in the presence of inversin (lower left). Twenty hours after transfection, 40 μg $ml^{-1}$ of cycloheximide (Cx) was added for 0, 4 or 8 h to HEK 293T cells to block protein synthesis; levels of Dvl1 were monitored by western-blot analysis. The reduction of Dvl1 levels in cells expressing inversin was blocked by the proteasome inhibitor ALLN (upper right). Increased ubiquitination of Dvl1 in the presence of inversin in Wnt3a-treated HEK 293T cells (lower right). (**b**) The mutation L493S destroys D-box 1 of inversin[2]. The mutant protein was expressed (middle) but did not block Dvl1-induced activation of the TOPFLASH promoter construct or reduce Dvl1 levels. (**c**) Inversin targets cytoplasmic Dvl1 for degradation. HEK 293T cells were transfected with Dvl1-HA and either FLAG-inversin or a control plasmid (FLAG-CD2AP; upper right). Western-blot analysis of the cytoplasmic and membrane fractions showed that only cytoplasmic Dvl1 was targeted by inversin. Equal protein loading was confirmed by γ-tubulin. Wild-type Dvl1 (Dvl1-HA) assumes a vesicular cytoplasmic staining pattern in transiently transfected HeLa cells, whereas Dvl1 containing a myristylation-palmitoylation consensus site (M/P-Dvl1-HA) assumes a diffuse cytoplasmic and plasma membrane localization (left). Inversin reduced wild-type Dvl1 (lower right) but had only a modest effect on Dvl1 containing a myristylation-palmitoylation consensus site. Reprobing with γ-tubulin (lower right) confirmed comparable protein loading.

Taken together, these results indicate that inversin inhibits canonical Wnt signaling upstream of the β-catenin degradation complex. Inversin forms a protein complex with dishevelled; immunoprecipitation of mouse Dvl1 immobilized inversin, whereas antibodies against Dvl1 precipitated inversin (**Fig. 2a**). This interaction was also demonstrated for endogenous proteins in MDCK cells, a renal tubular epithelial cell line (**Fig. 2a**). Studies using recombinant proteins showed that the C-terminal (but not the N-terminal) domain of inversin directly interacted with a glutathione S-transferase (GST) fusion protein containing the basic region and the PDZ domain of Dsh (**Fig. 2b**). Moreover, inversin colocalized with Dvl1 tagged with green fluorescent protein (GFP) in MDCK cells, and both proteins translocated to the plasma membrane with increasing confluency and polarization (**Fig. 2c**).

A consistent reduction of Dvl1 protein levels in cells expressing inversin prompted us to compare steady-state levels of Dvl1 in the presence and absence of inversin (**Fig. 3a**). Inversin shortened the half-life of Dvl1 and increased its ubiquitination, whereas ALLN, a proteasome inhibitor, blocked the degradation of Dvl1, suggesting that inversin targets Dvl1 for proteasome-dependent degradation (**Fig. 3a**). Inversin contains two destruction boxes (D-boxes), typically found in regulatory proteins with short half-lives[13]. D-box 1 interacts with APC2, a subunit of the multimeric anaphase-promoting complex known to regulate cell-cycle progression by selective degradation of proteins[14]. In an individual with nephronophthisis type II, the mutation L493S destroys D-box 1 (ref. 2). L493S mutant inversin failed to target Dvl1 for degradation and did not inhibit Dvl1-induced TOPFLASH activation (**Fig. 3b**). A myristylation-palmitoylation membrane anchor conferred resistance to inversin-mediated degradation (**Fig. 3c**), suggesting that inversin inhibits the canonical Wnt cascade by a new mechanism involving proteasomal degradation of cytoplasmic dishevelled.

Dishevelled is located at a decisive branch point between the canonical and the noncanonical Wnt pathways[10]. Both pathways require Wnt binding, Frizzled receptors and dishevelled, but they diverge downstream[11]. To test whether inversin has a role in the noncanonical Wnt pathway, we examined the role of inversin in convergent extension movements of *X. laevis* embryos. This assay system was used to show that β-catenin–independent noncanonical Wnt signaling controls cellular movements during gastrulation in vertebrates through a mechanism similar to the *Drosophila melanogaster* planar cell polarity pathway. RT-PCR analyses showed that endogenous inversin was expressed throughout all embryonic stages of *X. laevis* development, including gastrulation (**Supplementary Fig. 3** online). Overexpression of inversin, as well as knockdown of endogenous inversin by morpholino antisense oligonucleotides (inv-MO) on the dorsal side, impaired convergent extension movements in *X. laevis* embryos; mouse inversin rescued the phenotypic changes in a dose-dependent manner (**Fig. 4a**). Coinjection of inv-MO and β-galactosidase in dorsal marginal blastomeres resulted in failure of cells to condensate and converge at the midline during neurulation (**Fig. 4b**). To understand whether impaired convergent extension movements caused these abnormalities, we analyzed *X. laevis* animal cap assays. inv-MO inhibited activin-induced convergent extension movements of dorsal mesoderm and neural tissues and prevented the elongation of animal caps (**Fig. 4c**). RT-PCR analysis confirmed the expression of inversin in the animal hemisphere of early *X. laevis* embryos and showed that the failure to elongate was not due to a loss

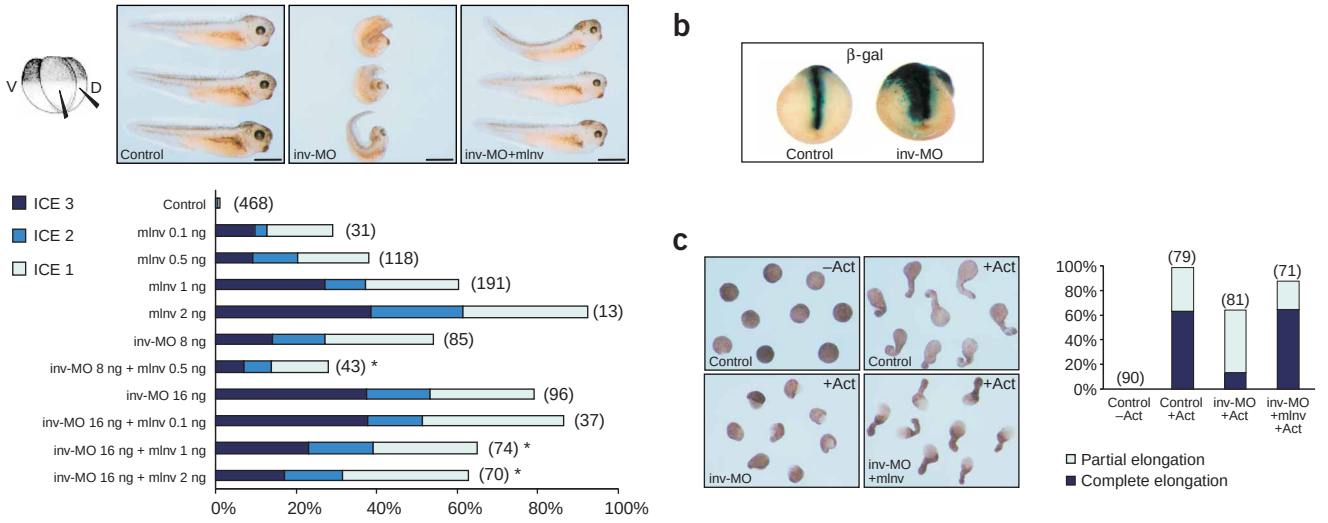


**Figure 4** Inversin is required for convergent extension movements in *X. laevis* embryos. (**a**) Knock-down of inversin by inversin morpholino antisense oligonucleotides (inv-MO) or overexpression of mouse inversin (mInv) impaired convergent extension movements of dorsal-mesodermal derived tissues during axis extension. Upper, reduced axis extension and dorsal flexure of embryos injected with 16 ng of inv-MO; these changes were rescued by mouse inversin RNA. Scale bars, 1 mm. Results are summarized in the lower panel (number of experiments per group is in parenthesis). The defects in convergent extension movements were scored as mild (ICE 1), moderate (ICE 2) or severe (ICE 3). (**b**) The dorsal blastomers of four-cell–stage embryos were injected with inv-MO and the lineage tracer β-galactosidase; embryos at late neurula stage were assayed for β-galactosidase activity *in situ*. Cells that inherited the inv-MO failed to converge in the midline and did not extend sufficiently in an anterior-posterior direction during neurulation. (**c**) inv-MO blocked elongation of activin-induced animal cap explants. Inhibition of activin (Act)-induced elongation by inv-MO was completely reversed by coinjection of mouse inversin RNA (mInv) not targeted by the morpholino oligonucleotide. Right, summary of the data; the numbers of animal caps of four independent experiments are shown above the bars.



of the dorsal mesoderm (**Supplementary Fig. 3** online). These findings suggest that inversin has a pivotal role in convergent extension movements.

We postulated that inversin-mediated inhibition of canonical Wnt signaling is essential for normal renal development. To test this hypothesis, we used the zebrafish model of cystogenesis induced by inversin depletion. Antisense morpholino oligonucleotides directed against the splice-donor site of the exon corresponding to nucleotides 2,259–2,921 of zebrafish inversin (invs-MO) initiate cyst formation in the pronephric duct in zebrafish embryos[2]. Diversin, structurally related to inversin, has a similar domain architecture with N-terminal ankyrin repeats and a modest degree of sequence conservation in the C-terminal domain (**Supplementary Fig. 4** online). Diversin inhibits canonical Wnt signaling and concomitantly controls gastrulation movements in zebrafish embryos[15]. The role of diversin in noncanonical Wnt signaling is further supported by its relationship to Diego, a *D. melanogaster* ankyrin repeat protein required for planar polarization of eye and wing epithelia[16]. Diversin inhibited the formation of renal cysts in zebrafish injected with invs-MO (**Fig. 5**).

This result suggests that cyst formation in the absence of inversin is caused by unopposed canonical Wnt signaling during permissive periods of renal development. Although canonical Wnt signaling is mandatory for mesenchymal-to-epithelial conversion and branching morphogenesis[17,18], constitutive activation of the canonical Wnt pathway leads to severe polycystic kidney disease during embryonic development[5,6]. The inhibition of canonical Wnt signaling by inversin was further exemplified by its effect on bozozok expression in zebrafish. Expression of bozozok (*boz*), a direct target of β-catenin–TCF activation[19,20], at 60% epiboly stage is restricted to the dorsal yolk syncytial layer, an area with high β-catenin–TCF activity[21]. In zebrafish embryos injected with invs-MO, *boz* expression extended to the lateral, ventral and animal yolk syncytial layer (**Fig. 5b**), indicating that enhanced β-catenin–TCF–mediated activation of *boz* prevailed over ventral BMP2b-dependent repression[20]. Overexpression of inversin affected cell morphology and delayed cell migration in epiboly (data not shown). Despite these effects on *boz* expression and gastrulation, however, overall zebrafish development proceeded relatively normally at the gross morphological level, except for body curvature, cardiac edema and kidney cysts.

The reversal of cyst formation by diversin also suggests that inversin has an essential role in noncanonical Wnt signaling. Although inversin targets cytoplasmic Dsh for degradation, inversin permits the accumulation of Dsh at the plasma membrane of polarized cells (**Fig. 2c**). In *D. melanogaster*, an analogous translocation of Dsh from the cytoplasm to the plasma membrane underlies the development of planar cell polarity in the wing[11]. Diego stabilizes the asymmetric distribution of Dsh-containing protein complexes at apical junctional complexes through interactions with the planar cell polarity pathway proteins Strabismus (Stbm) and Prickle (Pk)[22]. Notably, inversin shares with Diego the ability to bind Stbm and Pk (**Supplementary Fig. 5** online).

If tubular epithelial cells use noncanonical Wnt signaling to organize shape and function of the nephron, then how is the switch between Wnt pathways regulated? The onset of glomerular filtration and production of primary urine marks a new stage in the development of a nephron, exposing tubular epithelial cells for the first time to shear stress and bending of their primary cilium[23]. In inner medullary collecting duct (IMCD) cells, a flow rate equivalent to that of urine flow[24,25] upregulated expression of inversin (**Fig. 5p**). The flow-induced expression of inversin was accompanied by a modest reduction of β-catenin levels (**Fig. 5p**). Urine production begins markedly early in embryogenesis, long before fluid and

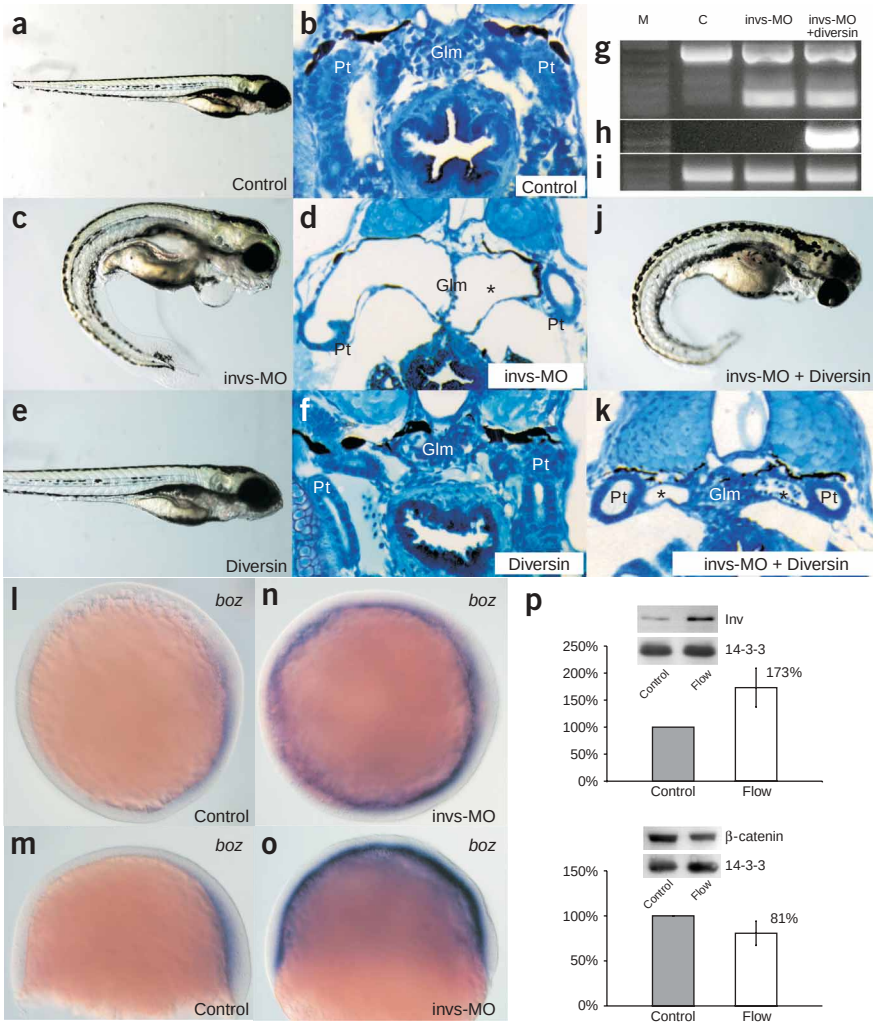


**Figure 5** Diversin rescues the renal cysts caused by inversin knockdown in zebrafish. (**a**) Embryos injected with a control morpholino oligonucleotide (MO) had normal morphology and development (173 of 176 injected embryos). (**b**,**c**) Histological sections of the pronephric kidneys at 4 d.p.f. showed the midline glomerulus (Glm) and pronephric tubule (Pt) of control animals (**b**), whereas embryos injected with invs-MO had ventral axis curvature (258 of 272 injected embryos; 95%; **c**). (**d**) The cystic glomerulus in invs-MO–injected 4-d.p.f. embryos had a flattened septum (asterisk) at the midline and a fluid-filled cyst lined with completely flattened epithelia. (**e**) 50 pg of mouse diversin mRNA alone had no marked effect on zebrafish development (282 of 312 injected embryos), whereas higher amounts resulted in progressive ventralization (ref. 15 and data not shown). (**f**) Histological section of 4-d.p.f. embryos injected with mouse diversin mRNA showed a normal pronephric kidney. (**g–i**) Molecular analysis of morpholino-targeted *invs* splicing defects. RT-PCR analysis of *invs* expression in 4-d.p.f. embryos injected with control morpholino generated a 746-bp *invs* fragment encoding the C-terminal domain of inversin (**g**; lane C, nucleotides 2,233–2,979; lane M, 1 kb plus markers, Invitrogen). Embryos injected with invs-MO (**g**; lane invs-MO; 4 d.p.f.) or invs-MO plus mouse diversin mRNA (**g**; lane invs-MO + diversin; 4 d.p.f.) analyzed with the same RT-PCR primers generated a 189-bp RT-PCR product, representing a C-terminal *invs* deletion allele. Some recovery of wild-type mRNA was observed at 4 d.p.f. (**h**) RT-PCR of mouse diversin mRNA in the same RNA samples as in **g** showed mouse diversin gene expression in animals coinjected with invs-MO and 50 pg of mouse diversin mRNA. (**i**) RT-PCR of β-actin mRNA in the same RNA samples as in **g**. (**j**) Coinjection of 50 pg mouse diversin mRNA with invs-MO rescued the cystic defects caused by inversin knockdown (261 of 284; 92%) but not the ventral axis curvature. (**k**) Histology section of 4-d.p.f. zebrafish, coinjected with invs-MO and mouse diversin mRNA, showed that diversin ameliorated cyst formation and partially rescued the glomerulus (Glm) and pronephric tubule structure (Pt). The fluid-filled cyst of the pronephric tubules is marked with an asterisk. (**l–o**) Knock-down of *invs* enhances canonical β-catenin signaling *in vivo*. (**l**,**m**) The expression of the Wnt target gene *boz* in control zebrafish embryos at 60% epiboly stage is restricted to the dorsal margin of the yolk syncytial layer. (**n**,**o**) *Invs* MO knockdown induces ectopic *boz* expression in the entire zebrafish yolk syncytial layer. (**p**) Inversin accumulates in response to flow. Using antiserum to inversin, the expression of inversin was determined by western blotting after 2 h of flow or without flow. Representative blots including the loading control 14-3-3 are shown. The mean value ± s.d. of seven independent experiments was determined using densitometry. Flow slightly decreased cytoplasmic β-catenin levels. Control cells were not exposed to flow. Both changes were statistically significant ($P < 0.05$).



electrolyte balance is required for homeostasis[26]. It is therefore tempting to speculate that urine flow terminates canonical Wnt signaling to facilitate β-catenin–independent Wnt pathways, perhaps to endow tubular epithelial cells with the spatial information important to maintain the genetically determined tubular geometry. Lack of functional inversin in *inv*/*inv* mice or individuals with nephronophthisis type II causes developmental defects due to unopposed canonical Wnt signaling that represses terminal differentiation of tubular epithelial cells and ultimately leads to renal cyst formation.

## METHODS

**Reagents and plasmids.** We used FLAG-tagged versions of full-length inversin as previously described[2]. We generated truncated forms of inversin by PCR and standard cloning techniques. Mouse hemagglutinin (HA)-tagged Dvl1 was provided by P. Salinas (Imperial College, London, UK); GST-Dsh-D6PDZ encoding amino acids 152–394 of *D. melanogaster* dishevelled, by K. Wharton Jr. (University of Southwestern Texas, Dallas, USA); and HA-diversin, by W. Birchmeier (Max-Delbrück Center, Berlin, Germany). For *X. laevis* embryo microinjections, we subcloned mouse inversin digested with *Eco*RI and *Xho*I into pXT7-derived expression vectors. We generated the mutation L493S in the inversin sequence by Quickchange site-directed mutagenesis (Stratagene). To generate membrane-bound Dvl1, we added the Lck myristylation-palmitoylation signal (MGCWCSSNPEDD) to the N terminus of Dvl1 by PCR and confirmed it by sequencing. All primer sequences are presented in **Supplementary Table 1** online. Plasmids for *X. laevis* Dsh, β-catenin and CK1ε were provided by S. Sokol (Mt. Sinai School of Medicine, New York, USA). Antibodies used in this study included mouse monoclonal antibody to HA (Roche Diagnostics), rabbit polyclonal antibody to HA (Covance or Sigma), antibody to 14-3-3 (Santa Cruz), antibody to β-catenin (Transduction Laboratories), M2 antibody to FLAG (Sigma) and antibody to γ-tubulin (Sigma).

Affinity-purified rabbit polyclonal antiserum to inversin was described previously[2]. Rabbit polyclonal antiserum against dishevelled-2 was provided by S. Sokol (Mt. Sinai School of Medicine, New York, USA).

**Subcellular fractionation.** To analyze cytoplasmic levels of β-catenin, we seeded HEK 293T cells in 10-cm plates, transiently transfected them with Dvl1-HA, FLAG-inversin or FLAG-CD2AP and then treated them as described[27].

**Coimmunoprecipitation and *in vitro* binding assay.** We carried out coimmunoprecipitations as described[27]. We transiently transfected HEK 293T cells with Dvl1-HA, HA-Akt, FLAG-inversin or FLAG-CD2AP using the calcium phosphate method. After incubating cells for 24 h, we washed them, pelleted them in phosphate-buffered saline (PBS) and lysed them in a buffer containing 20 mM Tris-HCl (pH 7.5), 1% Triton X-100, 25 mM NaF, 12.5 mM $Na_4P_2O_7$, 0.1 mM EDTA, 50 mM NaCl, 2 mM $Na_3VO_4$ and protease inhibitors. For endogenous immunoprecipitations, we lysed MDCK cells with the same buffer. After centrifugation (at 15,000 *g* for 15 min at 4 °C) and ultracentrifugation (at 100,000 *g* for 30 min at 4 °C), we incubated cell lysates containing equal amounts of total protein for 1 h at 4 °C with the appropriate antibody and then incubated them with 40 μl of protein A–sepharose beads for ~2 h. In some experiments, we used beads coupled to antibody to FLAG (Sigma). We washed the beads washed extensively with lysis buffer and resolved bound proteins by 10% SDS-PAGE. For the *in vitro* binding assay, we generated $^{35}$S-methionine–labeled full-length and truncated inversin using the Promega TNT system in accordance with the instructions of the manufacturer, incubated them with GST-Dsh-D6PDZ and GST alone and immobilized them using glutathione-Sepharose beads in a buffer containing 20 mM Tris-HCl (pH 7.4), 200 mM NaCl and 1 mM EDTA. We washed the beads with the same buffer and analyzed bound proteins by SDS-PAGE. Radiolabeled protein was detected by autoradiography.

**MDCK and HeLa cell transfections and immunocytochemistry.** We transfected MDCK cells with 2 μg of Dsh-GFP (provided by J. Axelrod, Stanford University, Palo Alto, California, USA) using the Amaxa Nucleofection system and cultured them in G418-containing medium to obtain cells overexpressing Dsh-GFP. For immunocytochemistry, we fixed cells at subconfluent and confluent states in 4% paraformaldehyde in PBS, permeabilized them in 0.2% TX-100 in PBS and blocked them in 3% bovine serum albumin with 2% fetal bovine serum. We detected inversin using an antiserum to inversin (provided by J. Nürnberger, University Hospital Essen, Essen, Germany)[28] in combination with Cy3-conjugated antiserum to rabbit (Jackson Immunoresearch). We analyzed samples with a Carl Zeiss LSM 510 confocal microscope. We transfected HeLa cells using Fugene6 and processed them for immunocytochemistry as described above.

**Luciferase assay.** We seeded HEK 293T cells in 12-well plates as previously described[27] and transiently transfected them with a TOPFLASH luciferase reporter construct, a β-galactosidase expression vector (provided by C. Cepko, Harvard Medical School, Boston, Massachusetts, USA) and vectors directing the expression of the proteins[27]. The total amount of DNA was 1.5–2.0 μg per well. Cells were serum-starved for 12 h, collected in cold PBS and lysed in 100 μl of reporter lysis buffer (Applied Biosystems) for 10 min at 4 °C. We centrifuged lysates at 14,000 r.p.m. for 5 min to remove insoluble material. We determined luciferase activity using a commercial assay system (Applied Biosystems) and normalized it to β-galactosidase activity to correct for transfection efficiency.

**Protein half-life and ubiquitination assay.** We treated HEK 293T cells with 40 μg ml$^{-1}$ cycloheximide for 0, 4 or 8 h to determine the half-life of Dvl1 in the presence or absence of inversin. To inhibit proteasome-dependent degradation, we incubated cells with 10 μM ALLN (Sigma) for 7 h before collecting them. We carried out ubiquitination assays as described[27]. Twenty-four hours after transfection, we lysed cells in 6 M guanidine-HCl, 0.1 M $Na_2HPO_4$, $NaH_2PO_4$ (pH 8.0) and 5 mM imidazole and sonicated them for 1 min. After centrifugation for 15 min at 4 °C, we precipitated FLAG-His-tagged Dvl1 from the cell lysate with nickel-nitrolotriacetic acid agarose (Qiagen) for 2 h at room temperature. We washed complexes with 8 M urea, 0.1 M $Na_2HPO_4$, $NaH_2PO_4$ (pH 6.3) and 0.01 M Tris (pH 8.0) and resuspended them in sample buffer. We used mouse monoclonal antibody to ubiquitin (Seromed) for immunoblotting. In some experiments, cells were serum-starved overnight and supernatant from Wnt3a-producing L cells (ATCC) was added 2 h before collection.

***X. laevis* embryo manipulations.** We injected one or two blastomeres at the four-cell stage with *in vitro*–transcribed mRNA (Ambion) or morpholino antisense oligonucleotides (inv-MO, 4–32 ng per embryo; GeneTools). We fixed embryos and scored them at tadpole stage 37/38 unless indicated otherwise. We scored secondary axes as absent (0), partial (only double tail and trunk; 1) or complete (secondary head structures (*i.e.*, eyes or cement gland); 2). We coinjected β-galactosidase or GFP RNA in equal amounts as control in a subset of embryos and observed no inhibition of Dsh- or CK1ε-induced axes. We scored phenotypic defects representing impaired convergent extension (ICE) as follows: ICE 1 (mild defects), <25% reduction of axis extension compared with uninjected embryos and mild dorsal flexure; ICE 2 (moderate defects), 25–50% reduction of axis elongation; ICE 3 (severe defects), shortening of >50%, head fused to tail or open neural folds. Normal control embryos (uninjected, injected with water or injected with nonfunctional RNA with equimolar amounts of β-galactosidase or GFP) had an ICE score of 0. An unrelated control morpholino (GeneTools; up to 32 ng per cell) did not induce convergent extension.

We dissected *X. laevis* animal caps at blastula stage 8 and cultured them in the presence of 7.5 ng ml$^{-1}$ of human recombinant activin A until control embryos reached developmental stage 18. We injected inv-MO (4–32 ng per cell) and RNA into the animal pole of four-cell–stage embryos. We scored elongation as partial (length/width ratio <2, incomplete proboscis) or complete (length/width ratio >2, full proboscis). We used unrelated morpholino (GeneTools) or unrelated RNAs (β-galactosidase, GFP) to exclude unspecific effects. We compared groups by Student's *t*-test, considering a *P* value <0.05 to be statistically significant.

For RT-PCR, we isolated RNA from *X. laevis* embryonic lysates of different developmental stages using the RNeasy kit (Qiagen). Primer sequences are available from the authors on request. We used ornithine decarboxylase as a control. In some embryos, we injected β-galactosidase (200–500 pg) together with the morpholino oligonucleotide to trace the cells that inherited the morpholino oligonucleotide. All experiments were approved by the institutional animal committee Regierungspräsidium Baden-Württemberg.

**Zebrafish embryo manipulations.** We used a morpholino (GeneTools) oligonucleotide directed against the splice-donor site of the exon corresponding to nucleotides 2,259–2,921 of zebrafish inversin (inv-MO) as described[2]. Primer sequences for invs-MO, mouse diversin and β-actin are available on request. We injected morpholinos into one- to two-cell–stage embryos in a solution of 0.25 mM morpholino, 200 mM KCl and 0.1% phenol red. The final cytoplasmic morpholino concentration was 1.5 μM. We carried out rescue experiments by coinjecting 50 pg of *in vitro*–transcribed mouse diversin mRNA with the morpholino oligonucleotide. This diversin concentration of 50 pg was determined in dose-response curves to exert minimal ventralizing effects while efficiently rescuing the invs-MO–mediated phenotype. For histological analysis, we embedded embryos in glycolmethacrylate (JB-4; Polyscience) at 4 d post-fertilization (d.p.f.) and stained them with methylene blue and azure II as previously described[2]. To examine expression of bozozok, we injected invs-MO (0.25 mM solution) targeted against the ATG of zebrafish *invs* into zebrafish (final cytoplasmic concentration 7.5 μM) and carried out *in situ* hybridization as described[19]. All experiments were approved by the institutional animal committee Regierungspräsidium Baden-Württemberg.

**Flow chamber assays.** We grew mouse IMCD cells on rectangular glass slides for at least 10 d in Dulbecco's modified Eagle medium and Ham's F12 medium containing fetal bovine serum, penicillin and streptomycin. To stimulate ciliated cells, we placed the glass slides in the laminar flow chamber with a flow path of 0.0254 cm in height and 1 cm in width (Glycotech) and sealed the chamber. We perfused the chamber with ringer solution with 10% fetal bovine serum at a flow rate of 25 ml h$^{-1}$ for 2 h at 37 °C. The flow rate was adapted to correspond to the reported tubular flow rate[26,27]. Control cells were not exposed to flow. For western-blot analysis, we scraped the cells off the slide, centrifuged them for 10 min at 13, 000 r.p.m. at 4 °C, resuspended them in lysis

buffer containing 150 mM NaCl, 50 mM Tris-HCl (pH 8.0), 4 mM EDTA and 1% TX-100 and then centrifuged them again. We determined protein concentration by Bio-Rad Protein assay (Bio-Rad). We used Scion Image software for densitometry.

*Note: Supplementary information is available on the Nature Genetics website.*

**ACKNOWLEDGMENTS**

We thank A. Schmitt for technical assistance; members of the laboratory of G.W. for discussions; E. Kim, K. Simons and S. Eaton for critically reading the manuscript; and P.A. Overbeek, P. Salinas, K. Wharton Jr., W. Birchmeier, H.J. Yost, S. Sokol, J. Axelrod and J. Nürnberger for providing materials. The work was supported by grants of the Deutsche Forschungsgemeinschaft.

**COMPETING INTERESTS STATEMENT**

The authors declare that they have no competing financial interests.

Received 24 December 2004; accepted 18 March 2005
Published online at http://www.nature.com/naturegenetics/

1. Watnick, T. & Germino, G. From cilia to cyst. *Nat. Genet.* **34**, 355–356 (2003).
2. Otto, E.A. *et al.* Mutations in INVS encoding inversin cause nephronophthisis type 2, linking renal cystic disease to the function of primary cilia and left-right axis determination. *Nat. Genet.* **34**, 413–420 (2003).
3. Mochizuki, T. *et al.* Cloning of inv, a gene that controls left/right asymmetry and kidney development. *Nature* **395**, 177–181 (1998).
4. Morgan, D. *et al.* Inversin, a novel gene in the vertebrate left-right axis pathway, is partially deleted in the inv mouse. *Nat. Genet.* **20**, 149–156 (1998).
5. Saadi-Kheddouci, S. *et al.* Early development of polycystic kidney disease in transgenic mice expressing an activated mutant of the beta-catenin gene. *Oncogene* **20**, 5972–5981 (2001).
6. Qian, C.N. *et al.* Cystic renal neoplasia following conditional inactivation of Apc in mouse renal tubular epithelium. *J. Biol. Chem.* **280**, 3938–3945 (2004).
7. Perantoni, A.O. Renal development: perspectives on a Wnt-dependent process. *Semin. Cell. Dev. Biol.* **14**, 201–208 (2003).
8. Guo, N., Hawkins, C. & Nathans, J. Frizzled6 controls hair patterning in mice. *Proc. Natl. Acad. Sci. USA* **101**, 9277–9281 (2004).
9. Moon, R.T., Bowerman, B., Boutros, M. & Perrimon, N. The promise and perils of Wnt signaling through beta-catenin. *Science* **296**, 1644–1646 (2002).
10. Wharton, K.A. Jr. Runnin' with the Dvl: proteins that associate with Dsh/Dvl and their significance to Wnt signal transduction. *Dev. Biol.* **253**, 1–17 (2003).
11. Veeman, M.T., Axelrod, J.D. & Moon, R.T. A second canon. Functions and mechanisms of beta-catenin-independent Wnt signaling. *Dev. Cell* **5**, 367–377 (2003).
12. Nelson, W.J. & Nusse, R. Convergence of Wnt, beta-catenin, and cadherin pathways. *Science* **303**, 1483–1487 (2004).
13. Zachariae, W. Destruction with a box: substrate recognition by the anaphase-promoting complex. *Mol. Cell* **13**, 2–3 (2004).
14. Morgan, D. *et al.* Expression analyses and interaction with the anaphase promoting complex protein Apc2 suggest a role for inversin in primary cilia and involvement in the cell cycle. *Hum. Mol. Genet.* **11**, 3345–3350 (2002).
15. Schwarz-Romond, T. *et al.* The ankyrin repeat protein Diversin recruits Casein kinase Iepsilon to the beta-catenin degradation complex and acts in both canonical Wnt and Wnt/JNK signaling. *Genes Dev.* **16**, 2073–2084 (2002).
16. Feiguin, F., Hannus, M., Mlodzik, M. & Eaton, S. The ankyrin repeat protein Diego mediates Frizzled-dependent planar polarization. *Dev. Cell* **1**, 93–101 (2001).
17. Stark, K., Vainio, S., Vassileva, G. & McMahon, A.P. Epithelial transformation of metanephric mesenchyme in the developing kidney regulated by Wnt-4. *Nature* **372**, 679–683 (1994).
18. Majumdar, A., Vainio, S., Kispert, A., McMahon, J. & McMahon, A.P. Wnt11 and Ret/Gdnf pathways cooperate in regulating ureteric branching during metanephric kidney development. *Development* **130**, 3175–3185 (2003).
19. Leung, T., Soll, I., Arnold, S.J., Kemler, R. & Driever, W. Direct binding of Lef1 to sites in the boz promoter may mediate pre-midblastula-transition activation of boz expression. *Dev. Dyn.* **228**, 424–432 (2003).
20. Imai, Y. *et al.* The homeobox genes vox and vent are redundant repressors of dorsal fates in zebrafish. *Development* **128**, 2407–2420 (2001).
21. Schneider, S., Steinbeisser, H., Warga, R.M. & Hausen, P. Beta-catenin translocation into nuclei demarcates the dorsalizing centers in frog and fish embryos. *Mech. Dev.* **57**, 191–198 (1996).
22. Das, G., Jenny, A., Klein, T.J., Eaton, S. & Mlodzik, M. Diego interacts with Prickle and Strabismus/Van Gogh to localize planar cell polarity complexes. *Development* **131**, 4467–4476 (2004).
23. Praetorius, H.A. & Spring, K.R. Bending the MDCK cell primary cilium increases intracellular calcium. *J. Membr. Biol.* **184**, 71–79 (2001).
24. Nauli, S.M. *et al.* Polycystins 1 and 2 mediate mechanosensation in the primary cilium of kidney cells. *Nat. Genet.* **33**, 129–137 (2003).
25. Liu, W. *et al.* Effect of flow and stretch on the [Ca2+]i response of principal and intercalated cells in cortical collecting duct. *Am. J. Physiol. Renal Physiol.* **285**, F998–F1012 (2003).
26. Friedberg, V. Studies on fetal urine secretion. *Gynaecologia* **140**, 34–45 (1955).
27. Kim, E. *et al.* The polycystic kidney disease 1 gene product modulates Wnt signaling. *J. Biol. Chem.* **274**, 4947–4953 (1999).
28. Nurnberger, J., Bacallao, R.L. & Phillips, C.L. Inversin forms a complex with catenins and N-cadherin in polarized epithelial cells. *Mol. Biol. Cell* **13**, 3096–3106 (2002).